12th International Conference on Applications of Statistics and Probability in Civil Engineering, ICASP12
Vancouver, Canada, July 12-15, 2015

Dynamic Response and Reliability of Tunnel under Earthquakes

Qingxia Yue
Associate Professor, Dept. of Civil Engineering, Shandong Jianzhu University, Jinan, China

Alfredo H-S. Ang
Research Professor, Dept. of Civil Engineering, University of California, Irvine, USA

ABSTRACT: The damages of tunnels under earthquakes showed that soil/rock deposits around a tunnel have significant effects on its response to earthquake excitations, including the effects of the spatial variability and correlation of the soil properties which may properly be modeled as a random field. This paper studied these effects through modeling the surrounding soil as a random field on the dynamic response of a tunnel. A 2D finite element model of the tunnel-soil system was examined and the corresponding random field was simulated by the stochastic harmonic function of the first kind. The results revealed that under the design earthquake, the static load effect will initially dominate but as the earthquake intensity increases, the earthquake influence will dominate. The reliabilities of a tunnel for the design limit-state function was considered. The equivalent extreme events were formulated for the limit-state function, from which the tunnel system reliability can be evaluated. The probability density evolution method (PDEM) was employed to calculate the reliability of the tunnel under its design limit-state when subjected to a strong earthquake. This shows that the tunnel is adequately designed by the existing Chinese code under the design earthquake.

The construction of underground tunnels is an essential component in the development of major infrastructure systems. In this regard, the nonlinear response analyses and reliability evaluations of tunnels under design and severe earthquakes are becoming significant problems in many parts of the world. During the Kobe earthquake of Japan in 1995, underground structures, such as the Daika subway station, were destroyed severely (Nishiyama et al., 2004), and in 1999, during the Chichi earthquake in Taiwan, 49 out of 57 mountain tunnels were destroyed to some extent (Wang et al., 2001). In 2008, during the Wenchuan earthquake in China, 56 tunnels were damaged and required retrofitting (Wang et al., 2009). Subsequent investigations and analyses revealed that the damages of the pertinent tunnels related closely to the geotechnical conditions of the surrounding soil/rock deposits.

In conventional tunnel response analyses, the soil properties are assumed to be the characterized values (usually the mean values) that were determined from laboratory tests of soil samples or on-site measurements. An analysis then proceed with these values in a deterministic manner yielding a solution that is dependent on the quality of the characteristic values. However, the soil or rock deposit around a tunnel is invariably non-homogeneous in properties due to its composition and deposition. These properties vary from point to point, and thus possess spatial correlations. The incorporation of random fields into engineering analysis allows the modeling of the spatially random soil, taking into account the correlation structures of the properties. Vanmarcke (1977) studied the two dimensional random soil profile and the scale of fluctuation was adopted to represent the spatial correlation; this study formed an important progress in random field model simulation of soil profiles. The present study models the soil around a tunnel as a random field and determines the response of

the tunnel and its reliability for the design limit-state under a specified strong earthquake.

1. RANDOM FIELD MODEL SIMULATION

The random field simulation usually requires field data processing to evaluate the spatial correlation function and adopt a numerical simulation procedure. The process is briefly introduced below, in which only the elastic modulus was assumed to be spatially correlated and random.

1.1. Site/laboratory Data Processing

The spatial variation of a soil property is conveniently expressed as the sum of a trend and a residual (De Groot and Baecher, 1993)

$$Y(X) = E(X) + \varepsilon(X) \tag{1}$$

in which $Y(\mathrm{X})$ is the soil property at location X; $E(\mathrm{X})$ is the trend function at X; and $\varepsilon(\mathrm{X})$ is the residual at X. The residual is assumed as a zero-mean stationary random field.

1.2. Elastic Modulus in Random Field

In the current study, the soil around a tunnel has been treated as a plasticity model with a spatially random elastic modulus and a constant Poisson's ratio.

The lognormal distribution was adopted for the generation of the elastic modulus field. The use of this distribution being constant with the knowledge that the elastic modulus should not have a negative value (Fenton and Griffiths, 2005). Accepting the use of this distribution, the elastic modulus field can be obtained through the transformation.

$$E_i = \exp(\mu_{\ln E} + \sigma_{\ln E} \cdot \mathrm{g}_i) \tag{2}$$

where E_i is the elastic modulus of the ith element; g_i is the corresponding standard Gaussian random field; and $\mu_{\ln E}$ and $\sigma_{\ln E}$ are the mean and standard deviation of lognormal E, which can be obtained using the following formula

$$\sigma^2_{\ln E} = \ln(1 + \sigma^2_E / \mu^2_E) \tag{3a}$$

$$\mu_{\ln E} = \ln(\mu_E) - \frac{1}{2}\sigma^2_{\ln E} \tag{3b}$$

Assume the correlation coefficient along depth z as

$$\rho(\tau) = \exp(-\frac{2|\tau|}{\delta}) \tag{4}$$

where τ is the spatial interval in the direction z and δ is the scale of fluctuation, which reflects the spatial correlation of the soil properties.

Assuming separable and independent correlation coefficients in the horizontal and vertical directions, the two dimensional correlation coefficient can be expressed as

$$\begin{aligned}\rho(\tau_1, \tau_2) &= \rho(\tau_1)\rho(\tau_2) \\ &= \exp(-\frac{2|\tau_1|}{\delta_1})\exp(-\frac{2|\tau_2|}{\delta_2})\end{aligned} \tag{5}$$

The correlation function is then,

$$R(\tau_1, \tau_2) = \sigma^2_{\ln E}\rho(\tau_1, \tau_2) \tag{6}$$

and the power spectral density can be obtained using the Wiener-Khinchine theorem as follows:

$$S(k_1, k_2) = \sigma^2_{\ln E}\left(\frac{2\delta_1}{\pi(4 + \delta_1^2 k_1^2)}\right)\left(\frac{2\delta_2}{\pi(4 + \delta_2^2 k_2^2)}\right) \tag{7}$$

where k_1, k_2 are the wave numbers and δ_1, δ_2 are the scales of fluctuations in the two directions, respectively. The correlation function or the power spectral density establishes the spatial probability structure of a Gaussian random field.

1.3. Generation of Elastic Modulus Field

There are various methods for generating the realizations of a random field, although the spectral method (Shinozuka and Deodatis, 1991) is the most widely used; however, the random variables are too many for any reliability analysis. In order to solve the problem, Chen et al.(2013) proposed the stochastic harmonic function of the first kind (SHF- Ⅰ) and second kind (SHF- Ⅱ) resulting in the random process being modeled with less weighted linear combinations of terms of the form $\cos(k_j x + \phi_j)$. This reduces the

dimension of the random variables, which is adopted in this paper for the reliability analysis.

For two dimensional problems, assume $Y(x_1, x_2)$ is the simulated random field. According to Chen et al. (2013), using the stochastic harmonic function of the first kind (SHI-I), $E(x_1, x_2)$ can be expressed as

$$E(x_1, x_2) = \sum_{j=1}^{N} A(\tilde{k}_{j,1}, \tilde{k}_{j,2}) \cos(\tilde{k}_{j,1} x_1 + \tilde{k}_{j,2} x_2 + \phi_j) \quad (8)$$

where the $\tilde{k}_j$ and ϕ_j are random wave numbers and random phase angles, respectively, the amplitudes $A(\tilde{k}_{j,1}, \tilde{k}_{j,2})$ are functions of $\tilde{k}_j$ and N is the number of components. In this case, the ϕ_j are independent and uniformly distributed random variables over [0, 2 π]. Suppose the support of $\tilde{k}_j$ is $[k_{i-1}^{(p)}, k_i^{(p)}]$, where the $k_i^{(p)}$ are different inner points over $[k_L, k_u]$, $i = 1, 2, ..., N$, $k_0^{(p)} = k_L$, $k_N^{(p)} = k_u$ and k_L and k_u are, respectively, the lower and upper cut-off frequency. Denote the PDF of $\tilde{k}_j$ following the distribution of the standardized shape of PSD.

$$f_{\tilde{\kappa}_j}(\tilde{\kappa}) = G_{\tilde{E}}(\tilde{\boldsymbol{\kappa}}) I\{\tilde{\boldsymbol{\kappa}} \in \Omega_j\} \Big/ \int_{\Omega_j} G_{\tilde{E}}(\tilde{\boldsymbol{\kappa}}) d\boldsymbol{\kappa} \quad (9)$$

and

$$A(\tilde{\boldsymbol{\kappa}}_j) = \sqrt{\frac{1}{2^{d-1}\pi^d} \int_{\Omega_j} G_{\tilde{E}}(\tilde{\kappa}) d\kappa} \quad (10)$$

where $f_{\tilde{k}_j}(\tilde{\kappa})$ is the PDF of $\tilde{\kappa}$, $I\{\cdot\}$ is the indicator function with the value 1 if the bracketed event is true and otherwise zero. $G_{\tilde{E}}(\tilde{\kappa})$ is the one-sided spectral density function of $E(x_1, x_2)$.

2. FINITE ELEMENT MODEL OF TUNNEL

2.1. Tunnel Information

The tunnel under consideration is a typical road tunnel for highways, located in Shandong province, China. The tunnel consisted of two lines that are 24m apart; the length of one line is 800m and the other line is 825m. Figure 1(a) shows the longitudinal geological conditions of one tunnel, with 5 boreholes for measuring the site data of the soil. The tunnel is shallow buried, with the maximum depth of 40m. For the sake of simplicity, a horizontal ground surface was assumed, with the average depth of 30m to the center of the tunnel. The detailed section is shown in Figure 1(b), with height and width of 10.01m and 11.50m, respectively. The lining is assumed to be 0.45m thick of shot-crete. Figure 1 (c) is the simplified model sketch.

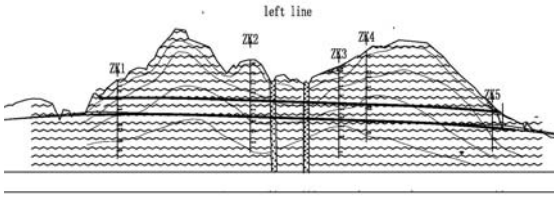

(a) The longitudinal section

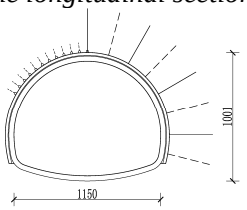

(b) Cross section of the tunnel (cm)

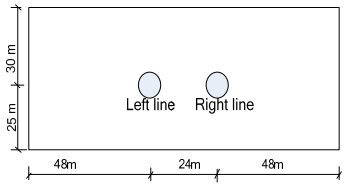

(c) Simplified calculation model

Fig.1 Tunnel information

2.2. Finite Element Model of Tunnel System

Plane strain condition is assumed for a 2D section of the tunnel. And as illustrated in Figure 2, the soil mass around the tunnel is modeled with a 2D finite element model consisting of four-node quadrilateral elements and the beam elements are adopted for the tunnel; the mesh size of the near field soil and the tunnel is about 1m and the far field soil is 2m. The separation and slip between the soil and tunnel are ignored

at present. In order to reduce or eliminate reflections of earthquake waves from the boundaries of the finite model, the infinite elements are added to the finite element model on the three sides of the model, as shown in Figure 2.

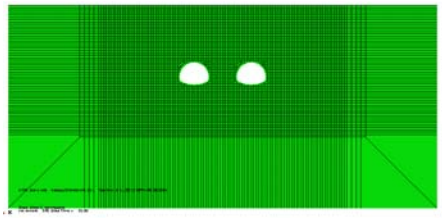

Fig. 2 The finite element model

2.3. Material Parameters

The Drucker-Prager constitutive model is adopted to simulate the plasticity of the soil, and the lining of the tunnel is assumed as elastic. The material parameters of the soil and lining are presented in Table 1. The elastic modulus of the soil is simulated as a random field.

Table 1 Material parameters of the soil and structure

parameters	soil	tunnel
Unit weight(kN/m^3)	*19.6*	*24*
Poisson's ratio	*0.30*	*0.15*
Young's modulus E (MPa)	*2200(mean)*	*200000*
friction angel(degree)	*50*	——
dilation angel(degree)	*5*	——
*k**	*1*	——
Coherence	*1.76*	——
yielding stress(MPa)	*20000*	——

* *k* is the ratio of the flow stress in tri-axial tension to the flow stress in tri-axial compression

The scale of fluctuation δ is important to describe the spatial variability. In this study, combining the site measured data and research results of Zhu and Zhang (2013) , the vertical and horizontal values of δ are 1m and 10m, respectively. The SHF- I (Eq. (8)) was then adopted in the numerical generation of the random field. One sample of the elastic modulus random field of the soil deposit, with dimensions of 120m by 55m in the horizontal and vertical directions, respectively, is shown in Figure 3 with a uniform finite element mesh size.

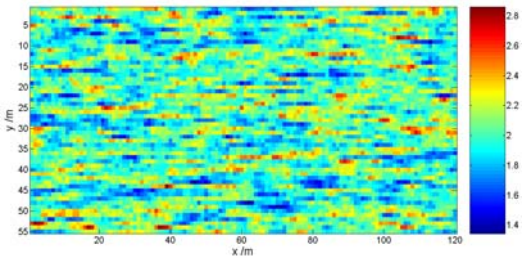

Fig. 3 One random field sample ($\times 10^9$ MPa)

2.4. Dynamic Input

In the present study, the acceleration time history recorded at Qingping station during the Wenchuan earthquake in 2008 was considered. The original seismic signal was characterized by a duration of 160 seconds with a maximum acceleration of 8.24m/s^2. For the sake of computational efficiency, the record between 30 and 65 sec, which is the strong vibration duration of the earthquake, was selected in the dynamic analysis. The horizontal component of the acceleration time history is presented in Figure 4. And the amplitude is adjusted to different fortification intensities according to China code for seismic design of buildings and the analysis cases are shown in Table 2. This seismic acceleration is the input from the base of the finite element model.

Table 2 Amplitudes of the earthquake acceleration

Case No.	*Seismic intensity*	*Acceleration amplitude (m/s^2)*	*Scale factor*
(1)	*Ⅶ frequently*	*0.35*	*0.0436*
(2)	*Ⅶ seldom*	*2.2*	*0.274*
(3)	*Ⅶ seldom*	*3.1*	*0.3892*
(4)	*Ⅷ seldom*	*4.0*	*0.4983*
(5)	*Wunchuan*	*8.24*	*1.0*

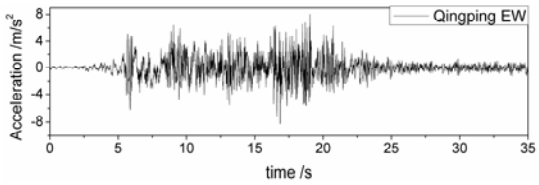

Fig.4 Acceleration time history of Qingping EW components (30-65s duration)

3. SEISMIC ANALYSIS RESULTS OF THE TUNNEL SYSTEM

3.1. Random Field Results

The actual tunnel located in the area of the seismic fortification intensity is Ⅶ. So the earthquake with Ⅶ frequently occurred was taken as an example, i.e. case (1) in Table 2. These results were obtained using the finite element software ABAQUS for the static and dynamic analyses shown in Figures 5 through 6.

Figure 5 is the axial stress of the tunnel. From the figure, it can be seen that the stresses at the corners of the tunnel are in tension at the top (inside) and in compression at the bottom (outside) of the tunnel lining.

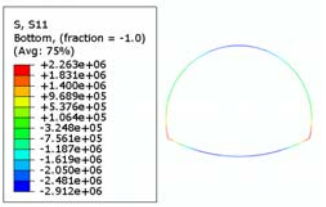

Fig. 5 The axial stresses in the tunnel

The distributions of the maximum and minimum envelops of the axial force N and bending moment M of one tunnel during the seismic event are shown in Figure 6. The results are presented as a function of the arc angle θ (also shown in Figure 6) and defined positive in the counter-wise direction of the arc.

From Figure 6, it can be seen that under the design earthquake, the gravity effects are the main effect. Maybe this is one reason for not considering the earthquake effects during the design of the tunnel. As a compression, the response of the tunnel under the Wenchuan earthquake amplitude, i.e. case (5) is illustrated in Figure 7.

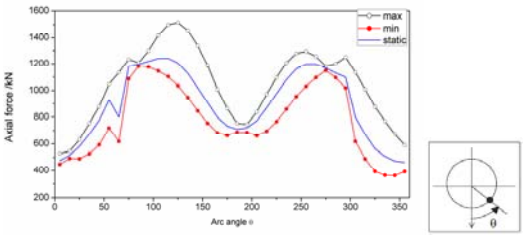

(a) Axial force along arc angle, θ

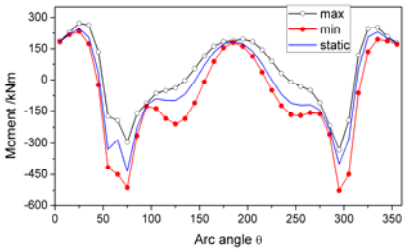

(b) Bending moment along arc angle, θ

Fig.6 Axial force and bending moment envelops around the tunnel (case(1))

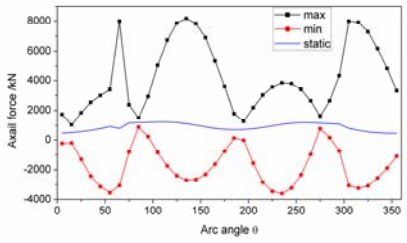

(a) Axial force along arc angle, θ

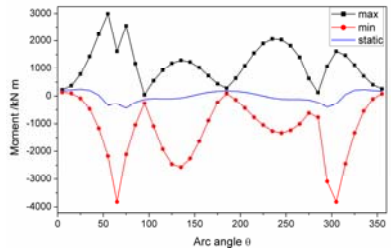

(b) Bending moment along arc angle, θ

Fig.7 Axial force and bending moment envelops around the tunnel (case (5))

From Figure7, it can be seen that as the earthquake intensity increases, the effects of the earthquake increase greatly and may become the dominant effects. It also showed that at the arc angle of about 60 degree and 300 degree, near

the corners of the tunnel, the axial force and bending moment are higher than elsewhere in the tunnel.

4. RELIABILITY EVALUATION OF THE TUNNEL

In the analysis of the reliability, the stochastic harmonic function proposed by Chen et al. (2013) was adopted for the simulation of the random field, with the advantage of using only a few terms (usually 6-10 cosine terms).

With the same tunnel system model as described above, and incorporating the recently developed probability evolution method (PDEM) (Li and Chen, 2004), the corresponding reliability is obtained with the equivalent extreme value events (Li et al., 2007a).

4.1. The Probability Density Evolution Method (PDEM)

To provide a brief synopsis of the probability density evolution method, the main formulas of the method are briefly outlined below.

According to Li and Chen (2008), the probability density evolution function equation is

$$\frac{\partial p_{X\Theta}(x,\theta,t)}{\partial t}+\dot{X}(\theta,t)\frac{\partial p_{X\Theta}(x,\theta,t)}{\partial x}=0 \qquad (11)$$

where $p_{X\Theta}(x,\theta,t)$ is the joint PDF of $X(x,\Theta)$; $\dot{X}(\theta,t)$ is the velocity of the structural response.

The initial condition of Eq.(11) is

$$p_{X\Theta}(x,\theta,t)\big|_{t=0}=\delta(x-x_0)\,p_{\Theta}(\theta) \qquad (12)$$

Eq.(11) can be solved with the initial condition of Eq.(12) using finite-difference method. The solution procedure may be described as follows:

(1) Select the representative points of the random variables. The selected points are $\theta_q(q=1,2,...,N_{sel})$, where N_{sel} is the total number of the representative points.

(2) Perform the response simulations based on the proposed random field model of the tunnel-soil system for each of the representative points.

(3) The finite-difference computation method (Chen and Li, 2005) is used to obtain the joint probability density function.

(4) Apply a numerical integration with respect to θ_q to obtain the numerical values of the PDF.

In the present paper, the number method (Li and Chen, 2007b) was adopted to generate the representative points, and 97 representative points of wave numbers $k_{j,1}$ and $k_{j,2}$, respectively, were generated with corresponding assigned probabilities. The phase angle ϕ_j is a random variable which is uniformly distributed in [0, 2 π].

4.2. PDEM-based Evaluation of the Extreme-value Distribution and System

4.2.1. Limit-state Functions

The limit-state function considered here is the design limit-state which is defined according to the *Code for Design of Road Tunnel* (JTG D70-2004) of China. For this limit-state, the cross section strength of the tunnel, as designed, can be divided into two types: (1) large eccentricity compression and (2) small eccentricity compression, in accordance with the relative compression height of the cross section, x, which is calculated as follows:

$$x=\frac{Nh_0-f_y^{'}A_s^{'}h_0+3.2f_yA_sh_0}{\alpha f_cbh_0+4f_yA_s} \qquad (13)$$

When $x\le 0.55h_0$, where h_0 is the effective height of the tunnel, it is defined as the large eccentricity compression, then the dimensionless design limit-state function is

$$Z1=\frac{KN}{R_wbx} \qquad (14)$$

or

$$Z1=\frac{KM}{R_wbx(h_0-x/2)+f_y'A_s'(h_0-a')} \qquad (15)$$

Whereas, when $x > 0.55h_0$, it is defined as small eccentricity compression. In this case, the dimensionless design limit-state function is

$$Z_2 = \frac{KM}{0.5R_a bh_0^2 + f_y A_S'(h_0 - a')} \quad (16)$$

where K is the safety factor; R_w and R_a are the bending and axial strength of concrete; f_y', A_s', a' and f_y, A_s, a, respectively, are the compression and tension reinforcement strength, the corresponding area and the distance of the bar to the bottom or top boundary of the section.

Based on the concept of the equivalent extreme-value event, the corresponding extreme-value event for the design limit-state can be formulated as

$$Z_{\max} = \max_{1 \le j \le m} (\max_{0 \le t \le T} (Z_1, Z_2)) \quad (17)$$

where j is the element number and T is the duration of the earthquake.

The dynamic reliability can then be obtained through one dimensional integration; namely,

$$R(T) = P\{Z_{\max} < 1\} = \int p_{Z_{\max}}(z)dz \quad (18)$$

4.3. Reliability Evaluation of the Tunnel

The reliability under the design limit-state, defined as not exceeding the design code-specified strength, is shown in Table 3. It can be seen that under case No.(1), which is the design earthquake condition, and the safety factor is also as required in the design code, the tunnel is adequately designed. As the amplitude of the earthquake increases, the reliability will decrease as expected. Also, when the amplitude of the earthquake is low, the large eccentricity compression limit-state, Eq. (15), will prevail and as the earthquake amplitude increases, the small eccentricity compression limit-state, Eq. 16, may dominate. Figure 8 is the PDF and CDF (cumulative probability density function) of the equivalent extreme-value event $Z_{\max}$.

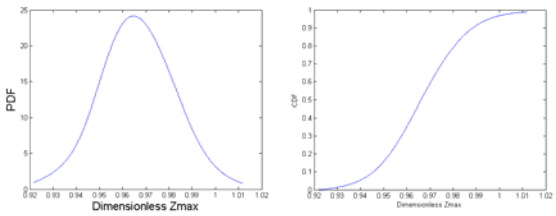

Fig. 8 The PDF and CDF of the ultimate limit-state function(case (4))

Table 3: Reliability of tunnel for design limit-state

Case No.	*thickness /m*	*Concrete /rebar*	*Safety factor K*	*Reliability* Pr
(1)	*0.45*	*C30/4Φ25*	*1.7*	*1.0*
(2)	*0.45*	*C30/4Φ25*	*1.0*	*0.9296*
(3)	*0.50*	*C30/5Φ25*	*1.0*	*0.9682*
(4)	*0.54*	*C30/5Φ25*	*1.0*	*0.9236*
(5)	*0.85*	*C40/5Φ25*	*1.0*	*0.8746*

5. CONCLUDING REMARKS

The soil/rock deposits around a tunnel clearly have spatial correlation and should be considered in the response analyses of the tunnel and in its reliability evaluations. This paper focused on the analysis of the tunnel-soil system with a random field model using the finite element method and determining the effects of the random field on the response and reliability of a specific tunnel subjected to a scenario earthquake. Based on this analysis, the following concluding remarks may be deduced.

(1)Soil and rock deposits invariably show spatial correlations -- for the accurate simulation of the random field, the site measurement or laboratory test of the soils/rocks should be used to define the soil/rock parameters.

(2) The analysis results show that the axial forces and bending moments around the tunnel arc angles are not uniformly distributed, and when the earthquake is not severe, the static load effect will have the main influence; whereas for severe earthquakes the effects of high intensity motions may dominate.

(3) Using the PDEM, the reliability evaluation of the tunnel can be obtained effectively.

(4) For the actual tunnel under consideration, its design against a design-specified earthquake is adequate and satisfy the design requirement. But as the amplitude of the earthquake increases, the reliability will decrease. Therefore, the tunnel may not be safe against collapse under strong earthquakes such as the Wenchuan event; the reliability against collapse is reported in a separate paper (Yue and Ang, 2015, accepted).

(5) The present study is based on a 2D approximation of the real tunnel problem. The authors recognize that the results obtained on this basis are approximate. To evaluate the degree of this approximation will require a 3D model of the tunnel-soil system; such a 3D study is currently in progress.

6. ACKNOWLEDGMENTS:

This work is supported by the Natural Science Foundation of China (Grant No. 51478253), Program for Changjiang Scholars and Innovative Research Team in University of China (No. IRT13075) and China Scholarship Council. Part of the research was undertaken when Qingxia Yue was a visiting scholar at the University of California, Irvine. These supports are gratefully acknowledged.

7. REFERENCES:

Chen JB, Sun WL, Li J, Xu J. Stochastic harmonic function representation of stochastic processes. *Journal of Applied Mechanics*, 2013, 80(1), 011001.

Chen, J. and Li, J. (2005). Difference method for probability density evolution equation of stochastic structural response. *Chinese Quart Mech*, 25(1), 22-28.

De Groot, D.J., and Baecher, G.B. (1993). Estimating autocovariance of in-situ soil properties. *Journal of Geotechnical Engineering*, 119(1), 147-166.

Fenton, G.A. and Griffiths, D.V. (2005). Three-dimensional Probabilistic foundation settlement. *Journal of Geotechnical and Geoenvironmental Engineering*, 131(2), 232-239.

Li, J., and Chen, J. (2004). Probability density evolution method for dynamic response analysis of structures with uncertain parameters. *Computational Mechanics.*, 34, 400-408.

Li, J., Chen, J., and Fan, W. (2007a). The equivalent extreme-value event and evaluation of the structural system reliability. *Structural Safety*, 29, 112-131.

Li, J., and Chen, J.(2007b). The number theoretical method in response analysis of nonlinear stochastic structures. *Computational Mechanics*, 39, 693-708.

Li, J. and Chen, J. (2008). The principle of preservation of probability and the generalized density evolution equation. *Structural Safety*, 30(1), 65-77.

Nishiyama, S., Kawama, I., and Haya, H. (2004). Analysis of the Cut and Cover Tunnels Damaged in the South-Hyogo Earthquake of 1995, *13th World Conference on Earthquake Engineering*, Canada, Paper No. 1511.

Yue Q., and Ang, A. H-S.(2015), Nonlinear Response and Reliability Analyses of Tunnels under Strong Earthquakes, *Int. J. Structures and Infrastructure Engineering,* (accepted)

Shinozuka, M., and Deodatis, G. (1991). Simulation of stochastic processes by spectral representation. *Applied Mechanics Reviews*, 44, 191-204.

Vanmarcke, E.H. (1977). Probabilistic modeling of soil profiles. *Journal of the soil Mechanics and Foundation Division, ASCE*, 103(GT11), 1227-1246.

Wang, W.L., Wang, T.T., Su, J.J., Lin, C.H., Seng, C.R. and Huang, T.H.(2001). Assessment of damage in mountain tunnels due to the Taiwan Chi-Chi Earthquake. *Tunneling and Underground Space Technology*, 16, 133-150.

Wang Z., Gao, B., Jiang, Y., and Yuan, S. (2009). Investigation and assessment on mountain tunnels and geotechnical damage after the Wenchuan earthquake. *Science in China Series E: Technological Sciences*, 52(2), 546-558.

Zhu, H., and Zhang, L.M. (2013). Characterizing geotechnical anisotropic spatial variations using random field theory. *Can. Geotech. J.* , 50, 723-734.